



Functionalized Titanium Nanoparticles Induce Oxidative Stress and Cell Death in Human Skin Cells

Patricia Brassolatti¹, Joice Margareth de Almeida Rodolpho¹, Krissia Franco de Godoy¹, Cynthia Aparecida de Castro¹, Genoveva Lourdes Flores Luna¹, Bruna Dias de Lima Fragelli¹, Matheus Pedrino¹, Marcelo Assis², Marcel Nani Leite³, Juliana Cancino-Bernardi⁴, Carlos Speglich⁵, Marco Andrey Frade³, Fernanda de Freitas Anibal¹

¹Laboratory of Inflammation and Infectious Diseases, Department of Morphology and Pathology, Federal University of São Carlos, São Carlos, São Paulo, Brazil; ²Center for the Development of Functional Materials, Department of Chemistry, Federal University of São Carlos, São Carlos, São Paulo, Brazil; ³Division of Dermatology - Wound Healing & Hansen's Disease Lab, Department of Internal Medicine, Ribeirão Preto Medical School, University of São Paulo, Ribeirão Preto, São Paulo, Brazil; ⁴Nanomedicine and Nanotoxicology Group, Physics Institute of São Carlos, University of São Paulo, São Carlos, São Paulo, Brazil; ⁵Leopoldo Américo Miguez de Mello CENPES/Petrobras Research Center, Rio de Janeiro, Rio de Janeiro, Brazil

Correspondence: Patricia Brassolatti, Departamento de Morfologia e Patologia UFSCar, Rod. Washington Luís, Km 235 Caixa Postal 676, São Carlos, CEP. 13565-905, SP, Brazil, Tel +551633518325, Fax +551633518326, Email patty.brassolatti@gmail.com

Purpose: Nanoparticles are resources of advanced nanotechnology being present in several products. Titanium dioxide nanoparticles are among the five most widely used NP currently expanding their benefits from the oil industry to the areas of diagnostic medicine due to their properties and small size. However, its impact on human health is still controversial in the literature. We aimed to evaluate the cytotoxicity of a new titanium NP functionalized with sodium carboxylic ligand (COOH^-Na^+) in human keratinocytes (HaCaT) and human fibroblasts (HDFn).

Methods: The physical-chemical characterization was performed by the transmission electron microscopy (TEM), dynamic light scattering (DLS) and zeta potential techniques, respectively. MTT and LDH assays were used to assess cytotoxicity and cell membrane damage respectively, ELISA to identify the inflammatory profile and, reactive oxygen species assay and cytometry to detect reactive oxygen species and their relationship with apoptosis/necrosis mechanisms.

Results: The results demonstrated a decrease in cell viability at the highest concentrations tested for both cell lines, but no change in LDH release was detected for the HaCaT. The cell membrane damage was found only at 100.0 $\mu\text{g/mL}$ for the HDFn. It was demonstrated that cytotoxicity in the highest concentrations evaluated for both cell lines for the 72 h period. The HDFn showed damage to the cell membrane at a concentration of 100 $\mu\text{g/mL}$ followed by a significant increase in reactive oxygen species production. No inflammatory profile was detected. The HaCaT showed apoptosis when exposed to the highest concentration evaluated and HDFn showed both apoptosis and necrosis for the same concentration.

Conclusion: Thus, it is possible to conclude that the cytotoxicity mechanism differs according to the cell type evaluated, with HDFn being the most sensitive line in this case, and this mechanism can be defined in a dose and time dependent manner, since the highest concentrations also triggered death cell.

Keywords: nanoparticle, titanium, cytotoxicity, human skin cells

Introduction

Nanotechnology is a multidisciplinary field that contemplates the union of science and technology whose function is to develop and manufacture materials at the atomic and molecular nanoscale comprised in the order of magnitude smaller than 100 nm.¹⁻³ Thus, a nanoparticle (NP) has specific properties that come from its small volume associated with its

extensive surface area, which in turn allows for both changes in thermal behavior, as well as greater resistance, solubility, conductivity, optical properties and catalytic activity.⁴

Due to these differentiated characteristics, nanoparticles gain not only the industrial field, including the automobile, petroleum, plastic and packaging industries, but also extend their benefits to the fields of medicine, medical, diagnostic and therapeutic purposes. In particular, titanium dioxide nanoparticles (TiO₂ NP) stand out for these applications due to their color, opacity, catalytic activity, photoactivity and biocompatibility. However, despite being considered biologically inert and with good versatility for applications in products from different areas and industrial segments, there are still issues related to its cytotoxic potential and real health risks when in contact with human beings, since the syntheses of these nanoparticles increasingly exploit components and reduced size.^{5,6}

The current literature presents controversies regarding the cytotoxic effects of titanium dioxide nanoparticles when in contact with the cellular environment since some authors report safety in its use without toxic evidence and others point out great concern, since they find cytotoxicity followed by inflammation mechanisms and cell death.⁷ Such difficulties can be associated both with the expressive variety of NP currently on the market and also with other characteristics, but no less relevant, such as its functionalization with chemical ligands, crystalline shape and size.⁷ Among the known crystalline forms of TiO₂ are anatase and rutile being the first described as chemically more reactive and likely more cytotoxic. Following this same path, with the advancement of nanotechnology resources and its ability to sharply synthesize, the production of NP of increasingly smaller size favored their inclusion in many products, but triggered a greater perspective of interaction in the cellular environment, thus inducing unwanted imbalances that could result in cytotoxicity.⁸⁻¹¹

Thus, it is evident that human beings and the environment are continually exposed to different types of NPs, especially titanium dioxide, since it is included in several products that emerge from paints and packaging to personal care products. However, its harmful effects resulting from this continuous and daily exposure are not fully understood. Titanium dioxide nanoparticles have different exposure pathways such as (1) inhalation, (2) ingestion, and (3) transcutaneous interaction. Regarding the skin tissue, it is known that exposure is daily and generally chronic, which has motivated several studies to evaluate its effects using human skin cells as *in vitro* models.¹²⁻¹⁶ However, it is worth mentioning that there is still an enormous difficulty in understanding its real toxic effects, due to the nanoparticles diversity as well as the scientific protocols used, which makes it difficult to compare the results obtained and the reasonability of its safety to human health.

Therefore, the work hypothesis is that a small NP when chemically functionalized is capable of minimizing its cytotoxic aspects increasing its safety both for those who synthesize them and for those who expose themselves daily in an indirect way. Therefore, the work aims to investigate a new titanium nanoparticle modified with sodium carboxylic ligands (COOH-Na⁺) in two different human skin cell line (keratinocytes and fibroblasts), in order to evaluate and define its cytotoxic potential.

Materials and Methods

Particle Characterization

Nanoparticle

The titanium dioxide nanoparticle evaluated in this study was developed due to an industry interest. Thus, after the TiO₂ NP was synthesized, it was sent to our research group by the Leopoldo Américo Miguez de Mello Research, Development and Innovation Center - CENPES/PETROBRAS. This new NP is composed of titanium dioxide with a surface modified with sodium carboxylic ligands (COOH-Na⁺).

Transmission Electron Microscopy (TEM)

A Jem-2100 LaB6 (Jeol) high resolution-transmission electron microscope (HR-TEM) with an accelerating voltage of 200 kV coupled with an INCA Energy TEM 200 (Oxford) was used to obtain larger magnifications and to clearly verify the TiO₂ samples. The samples were prepared by ultrasonic dispersion of the TiO₂ samples in culture medium, depositing small drops onto holed C coated Cu grids.

DLS and Zeta Potential

The dynamic light scattering (DLS) and zeta potential of the TiO₂ suspended in water and DMEM were evaluated using a Malvern spectrometer Nano-ZS (Malvern Instruments). The results are presented as mean ± SD resulting from three different measurements. Polydispersity index value (PDI) was also described.

Fluorescence Spectroscopy

For the characterization of absorption spectroscopy was used the UV-vis Cary 50 (Varian®) double-beam spectrophotometer with a 190–1100 nm spectrum, 1 cm plastic cuvettes and coupled to a microcomputer. Detection was made from 400 to 800 nm. The characterization of fluorescence spectroscopy was measurements using a Cary Eclipse Spectrofluorometer (Fluorescence Spectrophotometer - Agilent Technologies), in a 96-well white plate to reduce cross interference in luminescent assays. The acquisitions were made by stimulating the samples at 450 nm, collecting data from 470 to 800 nm.

In vitro Study

Cell Culture

HaCaT (human keratinocyte cell line) were acquired from the Bank of Cells of Rio de Janeiro and HDFn (human fibroblast cell line (Thermo Fisher Scientific (C0045C)) was acquired by the National Institute of Science and Technology of Optics and Photonics (INCT – INOF), of the Physics Institute of the University of São Paulo (USP), São Carlos campus and kindly assigned to our Research Group to carry out this study. These cell lines were chosen due to their representativeness and importance in the skin layers defined as epidermis and dermis, respectively. HaCaT cells and HDFn cells were grown in 75 cm² T flasks (Greiner, USA) containing Dulbecco's Modified Eagle Medium (DMEM) high Glucose medium (Sigma-Aldrich, USA), supplemented with 10% fetal bovine serum (FBS) (Hyclone, USA), 1% PEN/STREP Antibiotic (Gibco, USA) and 1% L-glutamine and Bicarbonate (Sigma-Aldrich, USA). T flasks were kept at 37 °C with 5% CO₂ in an incubator (Thermo Scientific, USA). TiO₂ NP were diluted in DEMEM medium at concentrations of 10, 100, 1000 and 2000 µg/mL for all analysis.

Cytotoxicity

The MTT (3-colorimetric tetrazolium (4,5-dimethylthiazol-2-yl) 2,5-diphenylbromide) method was used to evaluate the cell viability through mitochondrial activity.¹⁷ In 96-well plates, 4×10³ cells per well were inoculated for the HaCaT experiments and 5×10³ cells per well for the HDFn experiments. After cell adhesion in 96-well plate, the culture medium was removed, and NP of TiO₂ diluted in culture medium was added for each concentration of interest, which were: 10; 100; 1000; 2000 µg/mL in the experimental periods of 24, 48 and 72 h. For the negative control, only culture medium was used. For the positive control a dilution of 5% extran in culture medium was used. At the end of each experimental period, treatments with TiO₂ NP were removed and each well was washed twice with 1x sterile PBS. Then, 200 µL of MTT solution (0.5 mg/mL - Sigma-Aldrich) was added and maintained for 4 h in a 37 °C, 5% CO₂. After this period, 100 µL of DMSO (Synth) was added to dissolve the formazan crystals and perform the reading in a MultiSkan Go plate reader (Thermo-Fischer) at 570 nm. The cell viability was determined in percentage and compared with the control (Equation 1).

$$\% \text{ cytotoxicity} = \frac{\text{Experimental group}}{\text{Control group mean}} \times 100$$

LDH (Lactate Dehydrogenase)

Cell membrane damage was measured according to the CyQuant™ LDH Cytotoxicity Assay Kit (Invitrogen). After 72 h of exposure TiO₂ NP, 50 µL cell supernatant was added to a new 96-well plate and 50 µL of the Reaction Solution Kit was added and incubated for 30 min. The absorbance reading was measured at 490 nm and 680 nm on a plate spectrophotometer (Thermo Scientific™ Multiskan™ GO Microplate Spectrophotometer). To determine LDH activity, the values obtained at 680 nm of 490 nm were subtracted and the % cytotoxicity was calculated using the formula presented below.¹⁸

$$\% \text{ Cytotoxicity} = \frac{\text{Experimental group} - \text{Spontaneous LDH activity}}{\text{Maximum LDH activity} - \text{Spontaneous LDH activity}} \times 100$$

In which the Spontaneous LDH activity contained water and the Maximum LDH activity contained lysis solution.

Cellular Morphology

HaCat (4×10^3 cells/well) and HDFn (5×10^3 cells/well) cell morphology was evaluated after exposure to TiO_2 NP in a 96-well plate. After 72 h the exposure time, the cells were observed in an optical microscope Axiovert 40 CFL (Zeiss), whose images were captured using the coupled camera model LOD-3000 (Bio Focus) and analyzed by the Future WinJoeTM (v.2.0).

Cytokine Detection (TNF- α , IFN- γ , IL-6, IL-8 and IL-10)

TNF- α , IFN- γ , IL-6, IL-8 and IL-10 levels were measured using the ELISA quantification kit following the manufacturer's standards (BD Biosciences). HaCaT cell line, IL-8, IL-10 and INT- γ were evaluated. HDFn cell line, the cytokines IL-6, IL-10, TNF- α and INT- γ were evaluated. The choice of cytokines for each cell type was based on previous reports in the literature. The supernatant from the cell culture after the period of exposure to TiO_2 NP was collected and 50 μL of the well pool of this supernatant were added to a 96 well plate already sensitized with capture antibody and blocked with milk proteins 10%. Then, the secondary antibody conjugated with the enzyme peroxidase was added and after 2 h, the enzyme substrate (TMB) was added to the wells revealing the reaction. The absorbance reading was measured at 450 nm on a plate spectrophotometer (Thermo Scientific™ Multiskan™ GO Microplate Spectrophotometer) and concentrations were calculated from a standard curve for each sample.

Intracellular ROS Measurement

The production of reactive oxygen species (ROS) was detected using the fluorescent probe DCFH-DA (2', 7'-Dichlorodihydrofluorescein Diacetate) (Sigma-Aldrich).² After cultivation and the period of exposure to TiO_2 NP, the DCFH-DA probe was added to each well and the reaction occurred for 30 min. After that, the wells were washed with PBS 1x. The fluorescence emission reading was measured at 485-330 nm on a SpectraMax i3[®] plate spectrophotometer (Molecular Devices, CA, USA). The values obtained were transformed into percentages using the same formula previously mentioned in the MTT test (Equation 1). Images of the cells were also produced with the DCFH-DA probe using the ImageXpress Micro (Molecular Devices) equipment with a 20x objective lens.

Cell Apoptosis

Annexin V marker detection kit (PE and 7AAD - BD Biosciences) was used for the identification of cell death by apoptosis or necrosis. HaCaT (1×10^5 cells/well) and HDFn (8×10^4 cells/well) were seeded in a 24-well plate and exposed to NP TiO_2 for 72 h. After the period of exposure to TiO_2 NP, the plates were centrifuged at 1500 x and at 4 °C and washed with PBS 1x. Then the antibodies PE Annexin V and 7AAD (1:1) were added (1 μL /well in 1:10 binding buffer) and maintained for 15 min at room temperature without light. Then, the cells were scraped, removed from the plate and, then resuspended in microtubes with 300 μL of binding buffer. Analyses were performed in a flow cytometer (Accuri™ C6 BD Biosciences) with 10,000 events per port using FlowJo™ software version X (BD Biosciences).

Statistical Analysis

Homogeneity and Normality analyses were performed by the Levene and Shapiro–Wilk's tests, respectively. To determine the differences between the experimental groups and control groups, the one-way ANOVA test and Tukey's post hoc test were used. The values presented were considered significant when $p \leq 0.05$. For this purpose, the GraphPad Prism software was used. (Version 7.0 for Windows).

Table 1 DLS, Pdl and Zeta Potential Values of TiO₂ Nanoparticle in Different Medium

	DLS (nm)	Pdl	Zeta Potential (mV)
Water	2.78 ± 1.13	0.604 ± 0.082	-21 ± 2.3
DMEM	7.67 ± 0.41	0.491 ± 0.087	-10 ± 1.1

Abbreviations: NP, nanoparticle; TiO₂, titanium dioxide; TEM, transmission electron microscopy; DLS, dynamic light scattering; MTT, (3-colorimetric tetrazolium (4,5-dimethylthiazol-2-yl) 2,5-diphenylbromide); LDH, lactate dehydrogenase; ELISA, enzyme-linked immunosorbent assay; Pdl, polydispersity index value; PH, hydrogen potential; TiO₂ NP, titanium nanoparticle; µg/mL, microgram/milliliter; ROS, oxygen-reactive species; Nm, nanometer; TNF-α, tumor necrosis factor; IL-10, interleucina 10; IL-8, interleucina 8; IL-6, interleucina 6; LN cells, lymph node; HFF-1, hff1 human foreskin fibroblast; U87, human brain (glioblastoma astrocytoma); HaCaT cells, aneuploid immortal keratinocyte cell; HDFn cells, human dermal fibroblasts, neonatal.

Results

Particle Characterization

DLS and Zeta Potential

The results obtained by DLS and Zeta potential are shown in Table 1. Results of DLS showed significant differences of NP size due to the medium environment, which was also revealed by zeta potential values. In water, medium the average size values were 2.78 ± 1.13 nm, with zeta potential value to -21±2.3 mV. A great difference was observed in size, charge and polydispersity values when TiO₂ NP was dispersed in DMEM medium. The NPs increased in size with at least 5 nm and a decrease in their zeta potential value to -10 ± 1.1 mV. The latter was due to the protein corona formation in the surface of the nanoparticles, that growth a serum protein interface at the NP surface, increasing their size and charge.³

Transmission Electron Microscopy (TEM)

High Resolution Transmission Electron Microscopy (HR-TEM) was performed for the TiO₂ NP samples, in order to observe the agglomeration effects of the nanoparticles in contact with the culture medium (Figure 1). For the TiO₂-10 µg/mL sample, particles with good dispersibility and an average size of 12.1 nm are observed (Figure 1A). With the increase in concentration, observe the formation of agglomerates for samples TiO₂-100 µg/mL and TiO₂-1000 µg/mL, with average particle sizes of 15.4, 16.9 nm (Figure 1B and C). For the TiO₂-2000 µg/mL sample, a secondary structure of larger dimensions occurs with an average size of 29.3 nm (Figure 1D). In this way, the TiO₂ morphology is dependent on its concentration in the culture medium. In addition, all samples were indexed as tetragonal TiO₂ (anatase), with spatial group I41/amd due to the presence of the planes (101), (103) and (200) with interplanar distances of 3.52, 2.43 and 1.90 Å respectively.

Absorption and Fluorescence Spectra

Figure 2 shows the absorption and fluorescence spectra of TiO₂ NP diluted in water. When analyzed the absorption spectra (Figure 2A), was observed that the spectrum of the cuvette and the water remain as the same baseline and TiO₂ NP does not influence this spectrum in this wavelength range (400 to 800 nm). We also observed that the spectra of water and TiO₂ NP were superimposed and below the cuvette line. This behavior shows that light passing through the cuvette (without the presence of liquid or any sample) can suffer refraction, but when added to water or TiO₂ NP (diluted in water) this refractive index changes. Considering the fluorescence spectra of TiO₂ NP at concentrations of 100, 1000 and 2000 µg/mL, it is possible to observe that there is a spectrum formation that is probably attributed to the plate with these substances, so that TiO₂ NP did not interfere with fluorescence even considering the different concentrations. The fluorescence spectrum of TiO₂ NP diluted in DMEM medium was also analyzed. This showed similar behavior, that is, without promoting interference (Figure 2B).

In vitro Study

MTT

MTT is an initial assay to evaluate cytotoxicity through mitochondrial activity, mainly by the enzyme succinate dehydrogenase. The assay is based on the use of dehydrogenases by living cells that reduce soluble tetrazolium salts

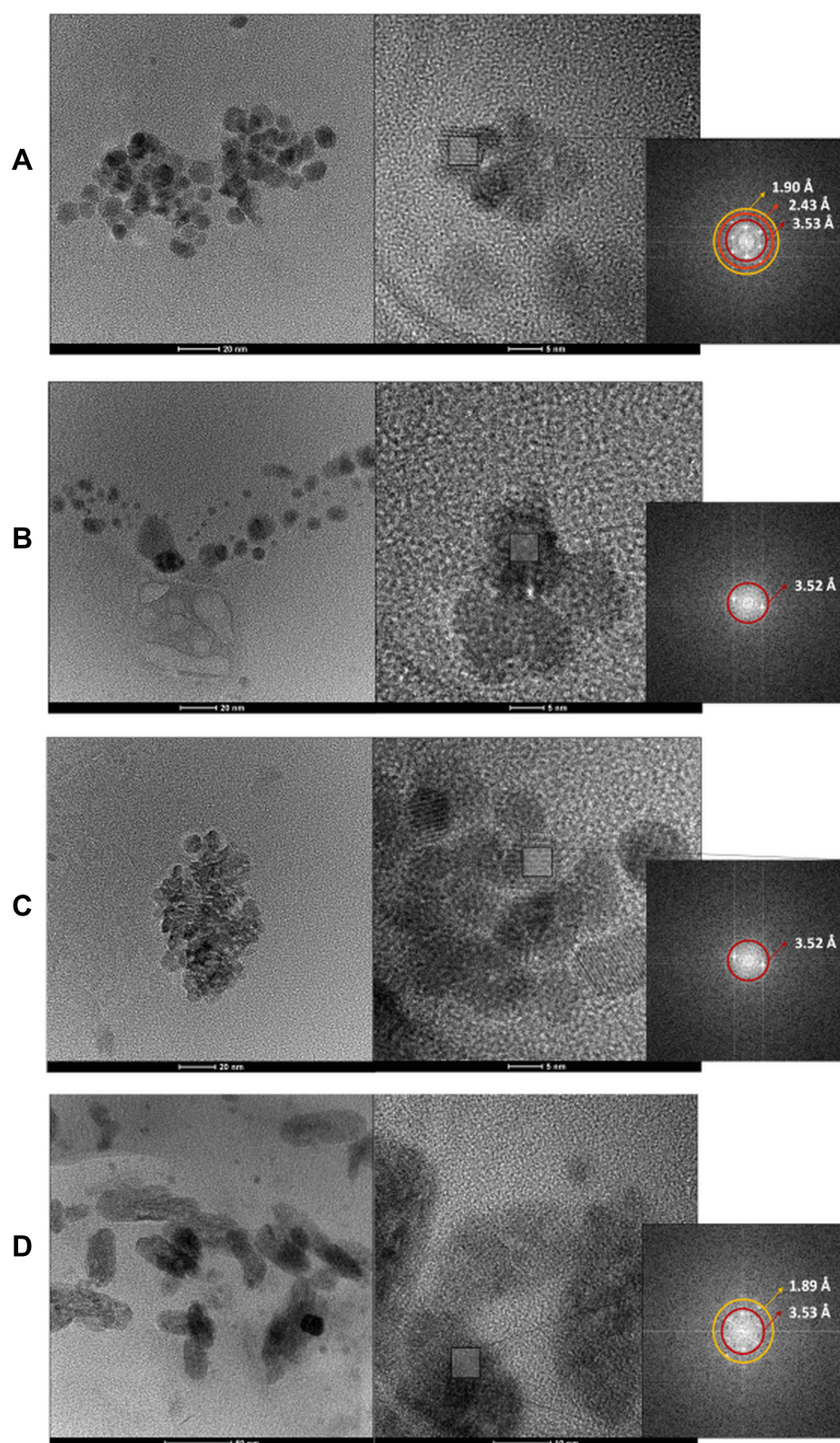


Figure 1 TEM and HR-TEM images. (A) TiO_2 -10 $\mu\text{g/mL}$, (B) TiO_2 -100 $\mu\text{g/mL}$, (C) TiO_2 -1000 $\mu\text{g/mL}$, (D) TiO_2 -2000 $\mu\text{g/mL}$.

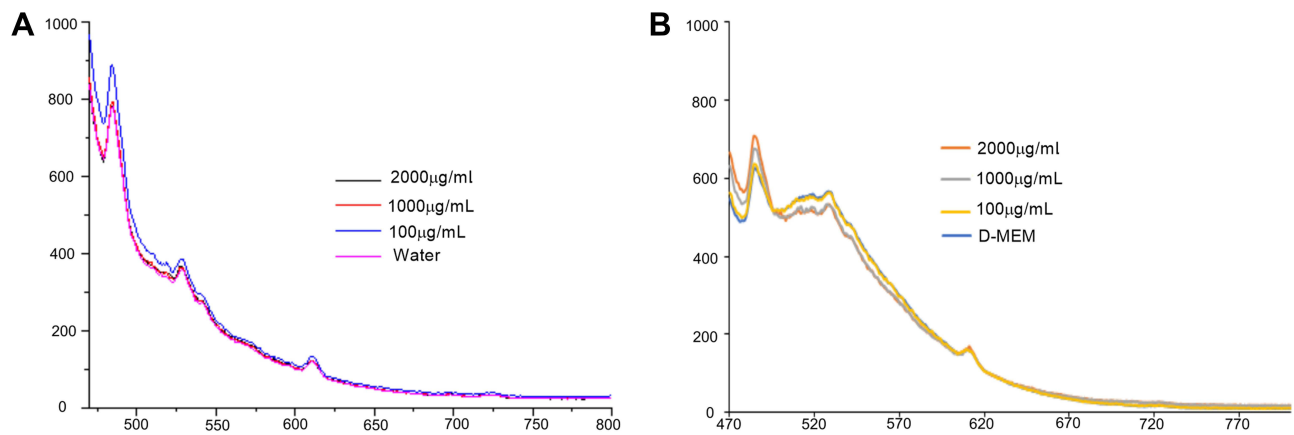


Figure 2 Absorption and fluorescence emission spectra of mixtures of TiO_2NP . (A) Absorption spectra of 2000, 1000 and 100 $\mu\text{g/mL}$ TiO_2NP in water. (B) Fluorescence emission spectra of TiO_2NP at concentrations of 100, 1000 and 2000 $\mu\text{g/mL}$.

(MTT) to insoluble formazan crystals, therefore, the absorbance value obtained regarding the dissolution of these crystals is proportional to the number of living cells. The results obtained indicate nanoparticle cytotoxic effects for both cell lines in the highest concentrations at 72-h. For HaCaT exposed to 1000 $\mu\text{g/mL}$ and 2000 $\mu\text{g/mL}$ of nanoparticles, there was a 40% and 30% reduction in cell viability, respectively (Figure 3A). For HDFn, the reduction was observed only at the concentration of 2000 $\mu\text{g/mL}$, showing a 37% reduction in cell viability (Figure 3C). Comparing the different time points used in the MTT assay, we defined 72 h as the period for further analysis of this work.

Lactate Dehydrogenase Assay

The results obtained in the evaluation of the LDH for the HaCaT did not show any significant difference in the groups evaluated (Figure 3B). However, in the HDFn, an increase of 15% in LDH release at a concentration 100 $\mu\text{g/mL}$ was observed when compared to the control, which might indicate cell membrane damage (Figure 3D).

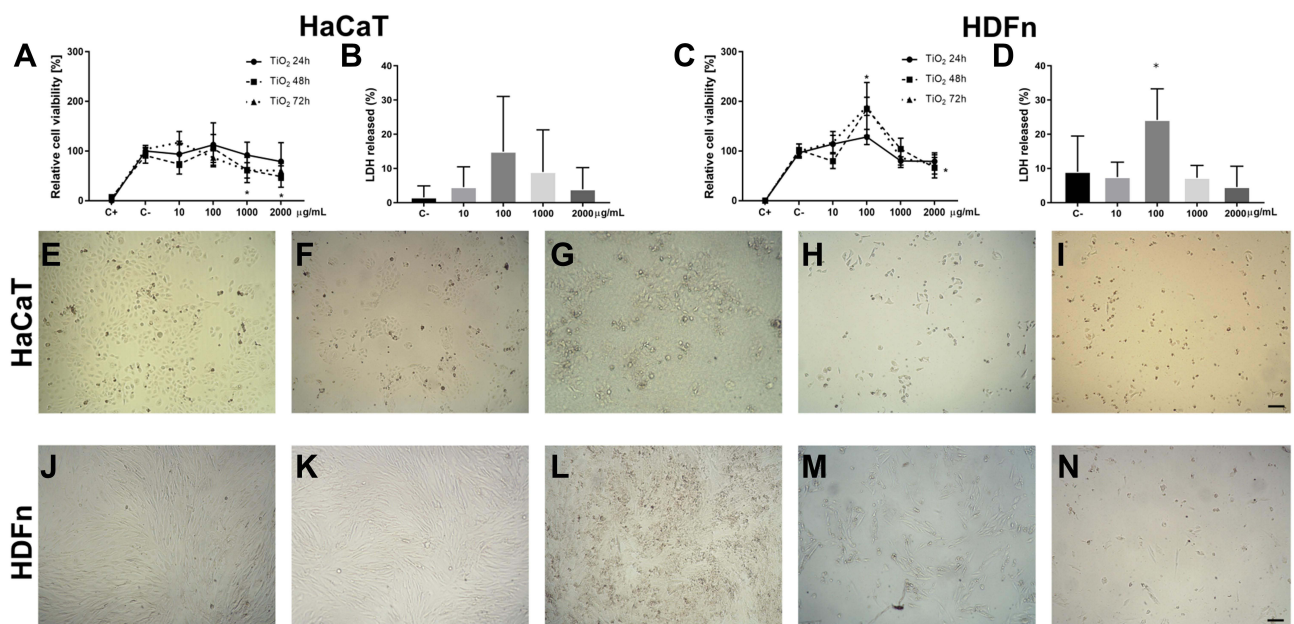


Figure 3 Cytotoxicity through mitochondrial activity and lactate dehydrogenase assay. (A) The cell viability of HaCaT cells after TiO_2 NP exposure for 24, 48, and 72 h; (B) release of LDH for HaCaT cells; (C) the cell viability of HDFn cells after TiO_2 NP exposure for 24, 48, and 72 h; (D) release of LDH for HDFn cells. Cell morphology of HaCaT and HDFn cells of exposure to different concentrations of TiO_2 NP for 72h. (E) Control HaCaT; (F) 10 $\mu\text{g/mL}$, (G) 100 $\mu\text{g/mL}$, (H) 1000 $\mu\text{g/mL}$ and (I) 2000 $\mu\text{g/mL}$; (J) control HDFn; (K) 10 $\mu\text{g/mL}$, (L) 100 $\mu\text{g/mL}$, (M) 1000 $\mu\text{g/mL}$ and (N) 2000 $\mu\text{g/mL}$. The statistical analysis was performed comparing the control group cell viability with TiO_2 NP treatments by two-way ANOVA (Dunnett's post-hoc); * $p < 0.05$.

Cellular Morphology

Morphologically keratinocytes are spindle-shaped and loosely compacted. Such characteristics are visible both in our control group and in the cells exposed to the lowest concentration of TiO₂. However, in the highest concentrations (1000 µg/mL and 2000 µg/mL) morphological changes are observed (Figure 3H and I), both in the reduction of cell content and also in cell density, presenting a greater thickening among them, losing the ability to form colonies characteristic of this cell line. Concentrations of 10 µg/mL and 100 µg/mL (Figure 3F and G) have similar morphology to the control (Figure 3E).

Regarding fibroblasts, it can be defined that they are extracellular matrix cells with a fusiform and elongated shape. When in contact with the TiO₂ NP, we observed that at the highest concentrations, significant changes in cell morphology were observed as the presence of stellate cells at a concentration of 1000 µg/mL and cells with a rounded shape at a concentration of 2000 µg/mL, showing that only a small part of the cellular content remained integrated in these concentrations (Figure 3M and N). It should be noted that at 100 µg/mL (Figure 3L) despite the cell showing similar morphological characteristics to the control, what is observed is a decantation of the TiO₂ NP at the bottom of the plate. Concentrations of 10 µg/mL (Figure 3K) have similar morphology to the control (Figure 3J).

Exposure Effect on Cytokine Production

Cytokine-mediated inflammatory response (pro-inflammatory) in HaCaT cells is shown in Figure 4. Regarding the levels of IFN-γ and IL-8, a reduction was observed when the keratinocytes were exposed to concentration 1000 µg/mL compared to the control (Figure 4A and B). In contrast, IL-10 levels showed a reduction when keratinocytes were exposed only to a concentration of 100 µg/mL (Figure 4C).

In turn, Figure 4D and E demonstrates the dosage of pro-inflammatory cytokines (IL-6 and IFN-γ) in the HDFn. The production of IL-6 did not differ in the concentrations at 10 to 1000 µg/mL. At 2000 µg/mL, a statistically significant decrease in IL-6 production was found when compared to the control (Figure 4E). Regarding IFN-γ, no production was detected at a concentration of 10 µg/mL, thus differing from the other experimental groups evaluated (Figure 4D). It should also be noted that the levels of IL-10 and TNF-α were measured for this cell line, but no expression was detected.

Intracellular ROS Measurement

ROS levels were measured by DCF-DA fluorescence probe as a detector of intracellular oxidant content in both cell lines, as shown in Figure 5. For the HaCaT in the concentrations (1000 and 100 µg/mL), exhibited increased fluorescence. In the concentrations evaluated (2000 and 10 µg/mL) the fluorescence intensity was not statistically different when compared to the control (Figure 5A). In the HDFn, the concentration of 100 µg/mL showed

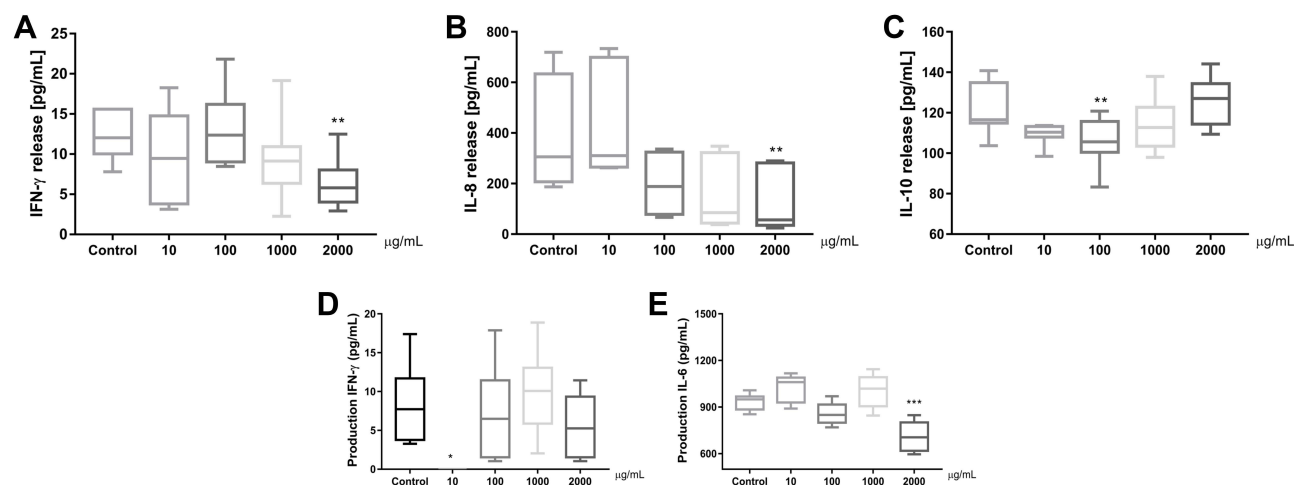


Figure 4 TiO₂ NP-induced cytokine production after the 72-exposure period. **(A)** Interferon-gamma (INT- γ), **(B)** interleukin-8 (IL-8), **(C)** I interleukin-10 (IL-10) when HaCaT were exposed to TiO₂ NP. **(D)** Interferon-gamma (INT- γ), **(E)** interleukin-6 (IL-6) when HDFn were exposed to TiO₂ NP. The statistical analysis was performed comparing the cytokine content among control group and TiO₂ NP treatments by one-way ANOVA (Tukey post-hoc); p * < 0.05, p ** < 0.01, p *** < 0.001.

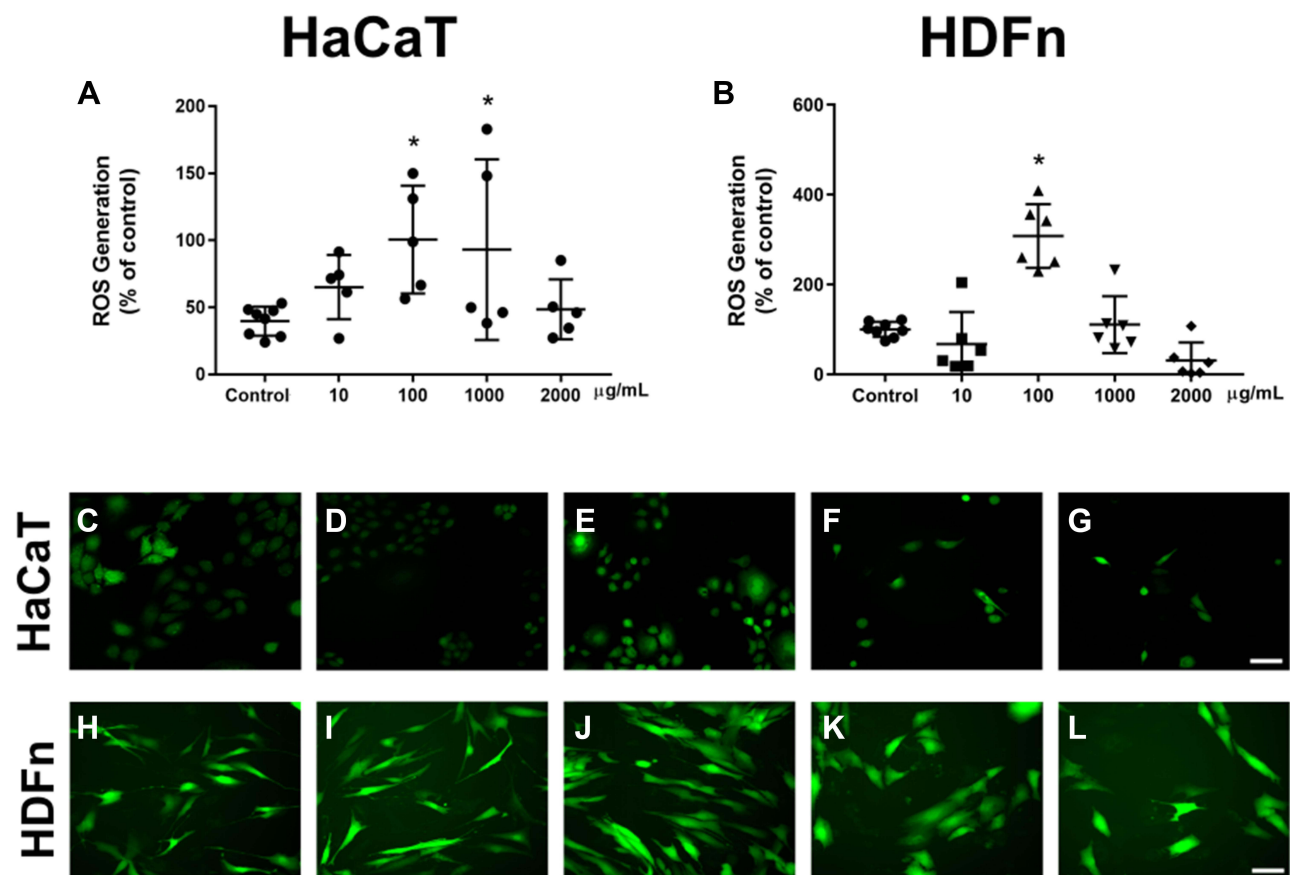


Figure 5 ROS production. Graphs and representative figures of fluorescence emitted after 72 hours of exposure in HaCaT cells and HDFn cells respectively. (A) Representative graph of ROS production for HaCaT cells and (B) representative graph of ROS production for HDFn cells. Fluorescence microscopy images of HaCaT and HDFn cells of exposure to different concentrations of TiO₂ NP for 72h. (C) Control HaCaT, (D) 10 µg/mL, (E) 100 µg/mL, (F) 1000 µg/mL and (G) 2000 µg/mL for the HaCaT cells. (H) Control HDFn, (I) 10 µg/mL, (J) 100 µg/mL, (K) 1000 µg/mL and (L) 2000 µg/mL for the HDFn cells. The statistical analysis was performed comparing the control group cell viability with TiO₂ NP treatments by one-way ANOVA (Tuckey post-hoc); * $p < 0.05$.

a statistically significant increase in fluorescence when compared to the control. The other groups evaluated for this cell line showed no significant difference when compared to the control (Figure 5B).

Cell Apoptosis

Apoptosis/necrosis evaluation of HaCaT and HDFn cells exposed to TiO₂ NP at 72 h was performed by the Annexin V assay using flow cytometry. Figure 6A shows the representative results of dot plot for both cell lines evaluated (HaCaT and HDFn) according to the Annexin V-PE/7AAD tag, respectively. The results obtained were expressed in % of fluorescence for each type of marker evaluated Annexin V PE/7AAD.

Figure 6B shows the results for the HaCaT cell line with a significant increase in apoptotic cells in the highest concentration of TiO₂ NP (2000 µg/mL) when compared to control group. At 100 µg/mL, there was a significant reduction in apoptotic and necrotic cells content when compared to the control group (Figure 6C). Figure 6G and H shows the % fluorescence of apoptotic and necrotic cells of the HDFn, with a significant increase in both apoptotic and necrotic cells to the concentration of 2000 µg/mL when compared to the control group.

The Heatmap graph shown in Figure 6D and I show the comparison between apoptotic and necrotic cells in 72 h of both cell lines through the average number of cells (HaCaT and HDFn). This chart shows the difference in colors (green represents the minimum and red the maximum) in the number of apoptotic and/or necrotic cells. Figure 6E, F, J and K illustrates the peak values given in % of apoptotic and necrotic cells of the groups evaluated in the form of histograms.

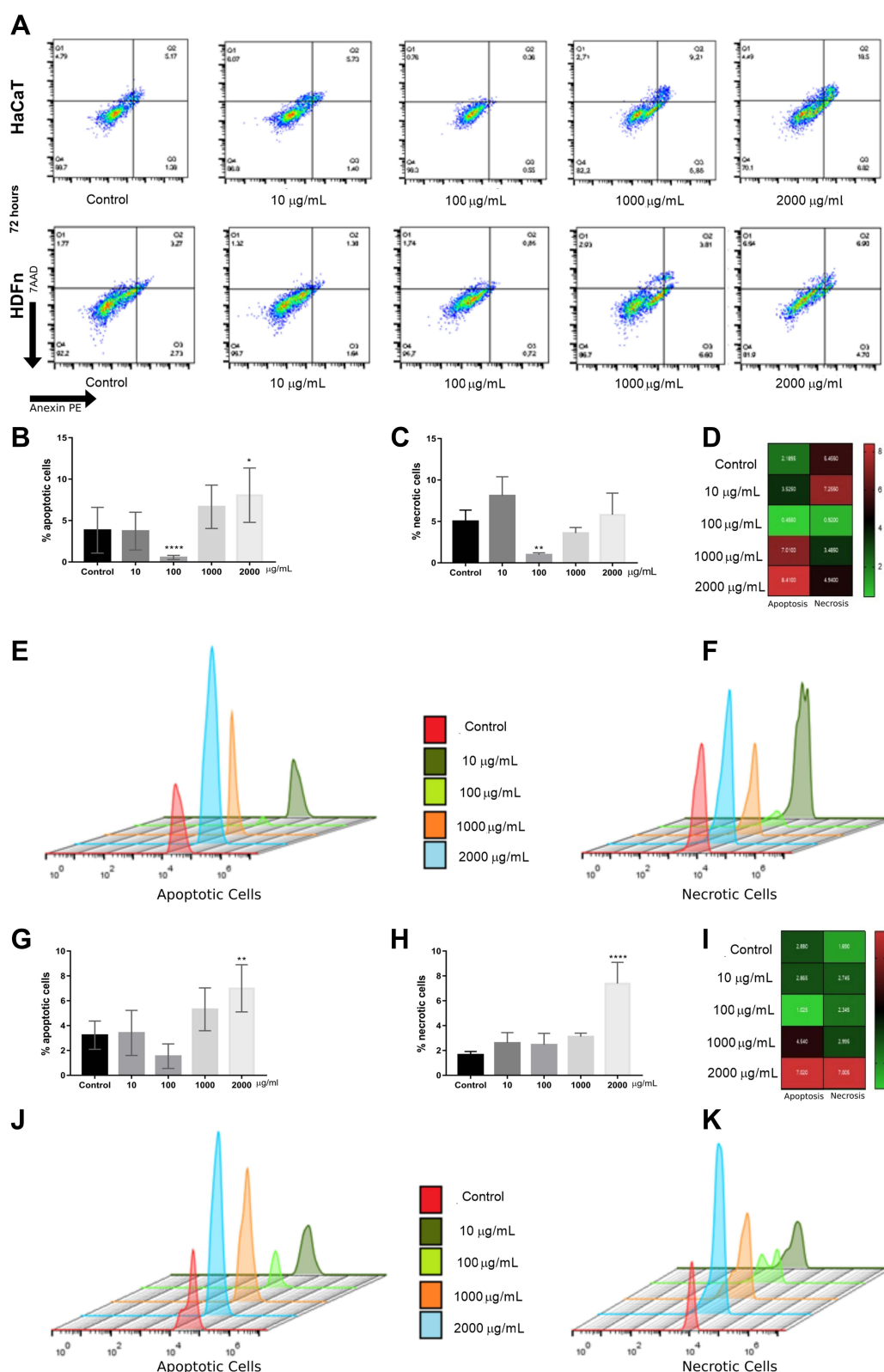


Figure 6 Apoptosis and necrosis by flow cytometry with PE markers annexin V and 7AAD. **(A)** DotPlot results referring to HaCat and HDFn cells respectively. **(B)** and **(C)** Representative graphs of apoptosis and necrosis respectively for HaCat cells. **(D)** Demonstration of apoptosis/necrosis by heatMap for HaCat cells. **(E)** Represent the peaks of apoptosis when HaCat cells were exposed to TiO_2 NP. **(F)** Represent the peaks of necrosis when HaCat cells were exposed to TiO_2 NP. **(G)** and **(H)** Representative graphs of apoptosis and necrosis respectively for HDFn cells. **(I)** Demonstration of apoptosis/necrosis by heatMap for HDFn cells. **(J)** and **(K)** represent the peaks of apoptosis and necrosis respectively when HDFn cells were exposed to TiO_2 NP. vs control; *p<0.05, **p<0.01, ****p<0.0001.

Discussion

Titanium dioxide is among the five most used nanomaterials by the industry, being present in the most diverse products of daily consumption.¹⁴ In view of this, this study evaluated the TiO₂ NP with carboxylate ligand in two human skin cell lines (keratinocytes and fibroblasts), in order to investigate its cytotoxic profile in the in vitro environment.

It is essential to highlight that for studies involving nanoparticles, prior knowledge of their main physical and chemical characteristics, such as size, surface area, charge and aggregation state, helps for understanding their behavior in the biological environment.¹⁵ It should be noted that for this study, measurements were performed using the fluorescence technique to verify if TiO₂ NP would exhibit optical properties and behavior during emission and excitation when diluted in water or in culture medium, which justifies that this NP does not promote any type of interference for in the wavelengths of the analyses proposed in this study.

In addition, currently many studies aim to achieve adaptations that meet the needs and demands of the industrial area, such as chemical modifications capable of reducing unwanted bioactivity, such as toxicity. Therefore, functionalized nanoparticles appear with different organic monolayers or chemical binders that exhibit different behaviors in relation to surface aggregation and adsorption in aqueous environments. The most applied chemical modification method involves the carboxyl group, as it is considered one of the most promising functional groups in chemistry and biochemistry, and for being able to reduce the bioactivity of certain nanoparticles of industrial interest.^{16,19}

In our study, characterization analyses indicated variations in hydrodynamic size and instability of TiO₂ NP dispersed in culture medium. In relation to TEM, it was possible to observe an increase in the size of NP according to the increase in nanoparticle concentration, being the largest hydrodynamic size found at 2000 µg/mL. Such aspects point to aggregation and agglomeration events that can be explained by the corona effect, which occurs when NP adsorb biomolecules such as proteins and lipids on its surface that can induce or reduce the formation of NP clusters. Generally, corona effect is influenced by NP size, incubation time, shapes, pH, ionic strength and negative zeta potential values.²⁰ The aspects most associated with the cytotoxic effect when in biological environment are the small size of the NP,² and its large surface area which enables chemical reactivity and its penetration into cells and tissues.⁶ Some studies also point out that the crystalline form of NP and its potential for agglomeration are directly associated with cytotoxic effects.^{4,13}

The use of titanium dioxide nanoparticles is considered relatively safe, chemically stable and non-cytotoxic.²¹ In general, non-photoactivated (UV light) titanium is considered a biocompatible material, however recent studies have been pointing out its cytotoxic potential in some cell culture such as human lymphocytes, keratinocytes, dermal fibroblasts and lung epithelial cells, not only when photoactivated but also in its natural state.^{9,22–25} Among the exposure routes described for titanium,²⁶ skin is one of the main routes for presenting direct contact, with quick access and great exposure, since TiO₂ NP is inserted widely in dermatological products.²⁷ In turn, the skin is a protective barrier that covers the entire length of the body efficiently, but its integrity can be impaired by several extrinsic factors such as injuries, burns and diseases, or by products and/or agents with inflammatory potential for topical use.²⁸ Thus, the need for biological evaluation of any type of chemical agent or NP of industrial interest is essential for safe use, since when in contact with the body it can trigger adverse effects depending on the condition of the type of contact.

Nanotoxicology studies indicate that titanium dioxide nanoparticles can trigger cytotoxic effects by different mechanisms, based on the unlike types and forms of structurally functionalized NP. Because of this, two interesting aspects can be observed: (1) functional biotechnological point of view, the smaller its size, the greater its stability and solubility, the greater its advantages for inclusion in different products. And (2) biological point of view, that remains focused on the interaction of this type of nanoparticle with the cellular environment, and often the reactive charge and the reduced size interfere in this good relationship leading to a mismatch that results in toxicity. Among the most investigated cellular mechanisms are cell viability, membrane damage, release of reactive oxygen species and apoptosis necrosis.^{9,22,29–33} Interestingly Ong et al 2017 and Lai et al 2008 report that the toxicity mechanism of a NP may be related to the cell type in which it is being evaluated, i.e, different cells and tissues may respond in different ways in front to the same type of NP.^{34,35}

According to one of the basic points from cytotoxicity study, Liu and Tang, 2019 addresses differences in relation to the term cell viability and cell metabolic activity, as several studies point to the assessment of viability by MTT.³⁶ However, we highlight that what is found in this methodology is related to mitochondrial activity and therefore, associated with metabolism. In our study, we observed a reduction in mitochondrial activity in both cells line tested at the highest concentrations at 72 h. Such results corroborate with the study by Montalvo-Quiros et al 2019 and Kim et al 2016 that also evaluated the cytotoxicity of a commercial NP TiO₂ (~ 25 nm) in human keratinocytes and observed that in 72 h the decrease in activity metabolic rate is directly related to increased concentration.^{22,37} In turn, Lai et al 2008 points out in their study the evaluation of NP TiO₂ <25nm in crystalline anatase form in fibroblasts, and report that there is a decrease in mitochondrial activity in all tested concentrations, with cytotoxicity becoming more evident in concentration of 100 µg/mL.³⁵ Already, Roslon et al 2018 observed that in the tested concentrations (10 to 200 µg/mL) in shorter periods of exposure (24 and 48 h), no cytotoxic profile was found.³⁸ Such findings suggest that the cytotoxicity of TiO₂ NP may be dose and time dependent.

The cell membrane is a bilayer composed mainly of phospholipids, responsible for selectively controlling the entry and exit of substances in the cell and maintaining the stability of the intracellular environment. In addition, the integrity of the cell membrane is a prerequisite for its optimal functioning. Under normal physiological conditions lactate dehydrogenase (LDH) is present in the cell cytoplasm and it is a great indicator of membrane damage.³⁶ Some authors correlate mitochondrial activity with membrane damage, in an inversely proportional mechanism. Lee et al 2018 demonstrate that MTT and LDH data are directly associated.²¹ Gholinejard et al 2019 confirmed the correlation when they investigated a commercial TiO₂ NP anatase and observed that the concentration of 100 µg/mL showed a decrease in cell viability with increased damage to the cell membrane.³⁹ This fact is contradictory to our findings, since in the concentration of 100 µg/mL for the fibroblast, an increase was detected in both techniques (MTT and LDH). In turn, the study by Lai et al 2008 reported that at the lowest concentrations, no changes were observed in this regard, but at the concentration of 50 µg/mL in 48 h of exposure, there was a moderate increase in LDH.³⁵ Regarding the evaluation in keratinocytes Yin et al 2012 points out that this damage was only found when in the presence of UV radiation, which is partially in agreement with our findings, since we did not find significant changes when HaCaT were exposed to TiO₂ NP.⁴⁰

In addition, another possible cell damage mechanism triggered by TiO₂ exposure may be associated with the metal ions released and their capacity to induce reactive oxygen species pathway activation, an expressively important pathway, which can subsequently trigger molecular actions such as activation of inflammatory cytokines. Shukla et al 2011 evaluated the production of free radicals using TiO₂ in aqueous suspension and observed a correlation between the generation of ROS and oxidative damage to DNA.⁴¹ Botelho et al 2014, described that TiO₂ is capable of increasing oxidative stress in gastric epithelial cells.⁴² In our study, an increase in reactive oxygen species was observed only at a concentration of 100 µg/mL when compared to the control. This fact becomes interest when we correlate it with the other analyses, because in this same concentration, no decrease in cell viability or damage to the cell membrane was detected. In this sense, the study by Tomankova et al 2015 points to an interesting discussion that should be taken into account, as they mention that TiO₂ NP are capable of inducing oxidative stress, but they point out that for human fibroblasts a lower production was detected when compared to other cell types.¹⁵ Furthermore, they mention that ROS production is not the main mechanism of cell damage caused by NP in general, but for NP TiO₂ this pathway plays an important role in relation to cell damage.

Another correlation that started to be explored is the investigation of the inflammatory profile. The study by Zhang et al 2018 evaluated the inflammatory profile of six different types of TiO₂ NP in human keratinocytes. The authors point out that there is an increase in IL-6 production in samples of two types of TiO₂ with different sizes, (32 nm and 27.3 nm) respectively, and an increase in TNF-α when cells were exposed to TiO₂ NP with sizes between 32 nm and 200 nm in high and medium concentrations. Furthermore, they report that there was no detection in the expression of IL-10 and IL-8. In particular, the authors point out that there is a probability that IL-8 was adsorbed by NP, especially at the highest concentrations evaluated.⁹ Contradictory, we found a decrease in IL-10 at a concentration of 100 µg/mL, and a lower production of IL-6 at the highest concentration tested, which does not corroborate previous reports, but it is noteworthy that at the highest concentration there was a significant decrease in cell viability and total number of cells. Interestingly, the study by Vanderbriel et al 2018 correlates the expression of cytokines with the type of crystal form of the NP evaluated. The authors demonstrate that anatase NP induced in LN cells, greater expression of TNF-α than pure rutile NP, but the same was

not found when IL-6 was evaluated.⁴³ Similarly, Gholinejad et al 2019 also investigated the expression of TNF- α and IL-6 when endothelial cells were exposed to crystalline NP anatase.³⁹ The results showed an increase in these proinflammatory cytokines dependent on the increase in NP concentration. The evaluation and comparison at the level of the type of NP and the concentration used demonstrates that our results do not corroborate previous findings, as we did not find the same inflammatory profile shown by the other studies. In this sense, it is essential to report that the cells presented in the studies have completely different profiles, which may provide differences in the sensitivity and expression profile of inflammatory cytokines, which may partially explain the variability of the results regarding this.

As the final route to the aforementioned biological processes occurs the cell death divided into two mechanisms, apoptosis and necrosis. Both mechanisms arise from a network of biochemical interactions that have overlaps depending on their main cause and/or the molecular events that precede them,⁴⁴ such as energy availability, damage to the genetic material or even the cell type involved. Generally, necrosis is a passive and uncontrolled process and apoptosis a more complex energy-dependent process.⁴⁵ In our study, we observed that both mechanisms (necrosis and apoptosis) were activated when cells were exposed to TiO₂ NP, but only at the highest concentration evaluated. In keratinocytes only apoptosis was detected and in fibroblasts both mechanisms (apoptosis/necrosis) demonstrating the overlapping mechanisms. The study by Roslon et al 2018 highlights that the results obtained by MTT were similar to those found in cytometry when evaluating apoptosis/necrosis, which corroborates our findings regarding the concentration of 2000 $\mu\text{g}/\text{mL}$ in both cell lines.³⁸ In contrast, the article by Kiss et al 2008 reported that for keratinocytes, the decrease in cell proliferation was not accompanied by cell death, but it emphasizes that in fibroblasts, the induction of apoptosis occurred in a dose and time-dependent manner.²⁸ Lai et al 2008 also evaluated the mechanisms of apoptosis/necrosis in U87 and HFF-1 cells and identified that both mechanisms increase according to the increase in the concentration of TiO₂ used³⁵ and that such reports are in agreement with the study by Park et al 2008.⁴⁶

With that, we emphasize that there is an immense difficulty in the investigation and comparison of the cytotoxic profile of NPs in general, since the variability found in the types of NP, isoforms, size and physicochemical characteristics are significant. In addition, there is currently no consensus on the ideal evaluation protocol so that these NPs can be considered toxic or non-toxic, as there are different routes of exposure, each research group uses a cell type and a methodology, which makes it even more difficult the eligibility of the risk of these NPs to human health. Therefore, this study suggests that there is much to be explored in the field of nanotechnology and further studies are needed in order to not only investigate the cytotoxicity profile of NPs of industrial interest, but also to complete a protocol that encompasses the main mechanisms of cellular interaction in order to establish a safe path in the comparison and prognosis for use in the different products.

Conclusion

Based on the results found in our study, we concluded that TiO₂ NP functionalized with the carboxyl ligand (COOH⁻Na⁺) is cytotoxic to human keratinocytes and fibroblasts at high concentrations, being able to induce cell membrane damage, oxidative stress and apoptosis. In addition, we emphasize that the concentration of 100 $\mu\text{g}/\text{mL}$ mentioned in many studies showed damage to the cell membrane and an increase in reactive oxygen species, which indicates a strong disturbance to the cellular environment in just 72 h of exposure. With these facts, we also indicate that only at very low doses (10 $\mu\text{g}/\text{mL}$) no cell alterations were observed. We also emphasize that, in view of this, there is a relative concern regarding the insertion of this type of NP in different daily consumption products, and therefore future studies are needed.

Acknowledgments

The authors acknowledge PETROBRAS for all the financial support during the execution of the work. We acknowledge the research group of Prof. Dr. Koiti Araki (University of São Paulo - USP/Brazil) for his collaboration in the synthesis of the tested nanoparticles and Biophotonics Laboratory from São Carlos Institute of Physics, University of São Paulo, for providing the fibroblasts used in this work and for support in the analysis of the fluorescence spectrum and physicochemical characterization. We also thank Prof. Dr. Márcia Regina Cominetti for support and collaboration in carrying out the flow cytometry technique and Prof. Dr. Elson Longo for assistance and support in the technique of Scanning Electron

Microscopy (TEM). We would also like to thank all the members of the Nano-PETROBRAS project team who indirectly assisted in this work.

Author Contributions

All authors made substantial contributions to conception and design, acquisition of data, or analysis and interpretation of data; took part in drafting the article or revising it critically for important intellectual content; agreed to submit to the current journal; gave final approval of the version to be published; and agree to be accountable for all aspects of the work.

Disclosure

The authors report no conflicts of interest in this work.

References

1. Dwivedi PD, Misra A, Shanker R, Das M. Are nanomaterials a threat to the immune system? *Nanotoxicology*. 2009;3:19–26. doi:10.1080/17435390802604276
2. Hussain S, Thomassen LC, Ferecatu I, et al. Carbon black and titanium dioxide nanoparticles elicit distinct apoptotic pathways in bronchial epithelial cells. *Part Fibre Toxicol*. 2010;7:1–17. doi:10.1186/1743-8977-7-10
3. Bostan HB, Rezaee R, Valokala MG, et al. Cardiotoxicity of nano-particles. *Life Sci*. 2016;165:91–99. doi:10.1016/j.lfs.2016.09.017
4. Browning CL, The T, Mason MD. HHS public access. *Ann Glob Health*. 2015;4:1–15.
5. Shi H, Magaye R, Castranova V, Zhao J. Titanium dioxide nanoparticles: a review of current toxicological data. *Particle Fibre Toxicol*. 2013;10. doi:10.1186/1743-8977-10-15
6. Xie G, Lu W, Lu D. Slightly damaged skin in vitro and in vivo. *J Appl Biomater Func Mater*. 2015;13:356–361.
7. Zhang LW, Monteiro-Riviere NA. Toxicity assessment of six titanium dioxide nanoparticles in human epidermal keratinocytes. *Cutan Ocul Toxicol*. 2019;38:66–80. doi:10.1080/15569527.2018.1527848
8. De Matteis V, Cascione M, Brunetti V, Toma CC, Rinaldi R. Toxicity assessment of anatase and rutile titanium dioxide nanoparticles: The role of degradation in different pH conditions and light exposure. *Toxicol in vitro*. 2016. doi:10.1016/j.tiv.2016.09.010
9. Zhang J, Song W, Guo J, et al. Cytotoxicity of different sized TiO₂ nanoparticles in mouse macrophages. *Toxicol Indust Health*. 2015;29:523–533.
10. Nohynek GJ, Lademann J, Ribaud C, Roberts MS. Grey Goo on the skin? Nanotechnology, cosmetic and sunscreen safety. *Crit Rev Toxicol*. 2007;37:251–277. doi:10.1080/10408440601177780
11. Jiang L, Jiang L, Xiong C, Su S. Colloids and surfaces B: biointerfaces improving the degradation behavior and in vitro biological property of nano-hydroxyapatite surface- grafted with the assist of citric acid. *Colloids Surfaces B Biointerfaces*. 2016;146:228–234. doi:10.1016/j.colsurfb.2016.05.062
12. Weihua W, Vriend CY, Wetmore L, et al. The effects of stress on splenic immune function are mediated by the splenic nerve. *Brain Res Bull*. 1993;30:101–105. doi:10.1016/0361-9230(93)90044-C
13. Lesniak A, Salvati A, Santos-Martinez MJ, et al. Nanoparticle adhesion to the cell membrane and its effect on nanoparticle uptake efficiency. *J Am Chem Soc*. 2013;135:1438–1444. doi:10.1021/ja309812z
14. Vance ME, Kuiken T, Vejerano EP, et al. Nanotechnology in the real world: redeveloping the nanomaterial consumer products inventory. *Beilstein J Nanotechnol*. 2015;6:1769–1780. doi:10.3762/bjnano.6.181
15. Tomankova K, Horakova J, Harvanova M, et al. Reprint of: cytotoxicity, cell uptake and microscopic analysis of titanium dioxide and silver nanoparticles in vitro. *Food Chem Toxicol*. 2015;85:20–30. doi:10.1016/j.fct.2015.10.012
16. Hamilton RF, Wu N, Xiang C, et al. Synthesis, characterization, and bioactivity of carboxylic acid-functionalized titanium dioxide nanobelts. *Part Fibre Toxicol*. 2014;11:1–15. doi:10.1186/s12989-014-0043-7
17. Mosmann T. Rapid colorimetric assay for cellular growth and survival: application to proliferation and cytotoxicity assays. *J Immunol Methods*. 1983;65:55–63. doi:10.1016/0022-1759(83)90303-4
18. Kumar P, Nagarajan A, Uchil PD. Analysis of cell viability by the lactate dehydrogenase assay. *Cold Spring Harb Protoc*. 2018;2018(6):465–468.
19. Shan Z, Yang WS, Zhang X, Huang QM, Ye H. Preparation and characterization of carboxyl-group functionalized superparamagnetic nanoparticles and the potential for bio-applications. *J Braz Chem Soc*. 2007;18:1329–1335. doi:10.1590/S0103-50532007000700006
20. Gebauer JS, Malissek M, Simon S, et al. Impact of the nanoparticle-protein Corona on colloidal stability and protein structure. *Langmuir*. 2012;28:9673–9679. doi:10.1021/la301104a
21. Lee SU, Lee JE, Kim SJ, Lee JS. Effects of titanium dioxide nanoparticles on the inhibition of cellular activity in human Tenon's fibroblasts under UVA exposure. *Graefes Arch Clin Exp Ophthalmol*. 2018;256:1895–1903. doi:10.1007/s00417-018-4091-9
22. Montalvo-Quiros S, Luque-Garcia JL. Combination of bioanalytical approaches and quantitative proteomics for the elucidation of the toxicity mechanisms associated to TiO₂ nanoparticles exposure in human keratinocytes. *Food Chem Toxicol*. 2019;127:197–205. doi:10.1016/j.fct.2019.03.036
23. Zdravkovic B, Zdravkovic TP, Zdravkovic M, Strukelj B, Ferk P. The influence of nano-tio2 on metabolic activity, cytotoxicity and abcb5 mRNA expression in wm-266-4 human metastatic melanoma cell line. *J B.U.ON*. 2019;24:338–346.
24. Bogusz K, Tehei M, Lerch M, Dou SX, Liu HK, Konstantinov K. TiO₂/(BiO)₂CO₃ nanocomposites for ultraviolet filtration with reduced photocatalytic activity. *J Mater Chem*. 2018;6:5639–5650.
25. Chang J, Lee C-W, Alsulimani HH, et al. Role of fatty acid composites in the toxicity of titanium dioxide nanoparticles used in cosmetic products. *J Toxicol Sci*. 2016;41:533–542. doi:10.2131/jts.41.533

26. Zeng C, Feng Y, Wang W, et al. The size-dependent apoptotic effect of titanium dioxide nanoparticles on endothelial cells by the intracellular pathway. *Environ Toxicol.* **2018**;33:1221–1228. doi:10.1002/tox.22628
27. Sha B, Gao W, Cui X, Wang L, Xu F. The potential health challenges of TiO₂ nanomaterials. *J Appl Toxicol.* **2015**;35:1086–1101. doi:10.1002/jat.3193
28. Kiss B, Br T, Czifra G, et al. Investigation of micronized titanium dioxide penetration in human skin xenografts and its effect on cellular functions of human skin-derived cells. *Exp Dermatol.* **2008**;17:659–667. doi:10.1111/j.1600-0625.2007.00683.x
29. Miyani VA, Hughes MF. EPA public access. *Cutaneous Ocular Toxicol.* **2018**;1–16. doi:10.1080/15569527.2016.1211671
30. Periasamy VS, Athinarayanan J, Al-Hadi AM, et al. Identification of titanium dioxide nanoparticles in food products: induce intracellular oxidative stress mediated by TNF and CYP1A genes in human lung fibroblast cells. *Environ Toxicol Pharmacol.* **2015**;39:176–186. doi:10.1016/j.etap.2014.11.021
31. Niska K, Zielinska E, Radomski MW, Inkielewicz-Stepniak I. Metal nanoparticles in dermatology and cosmetology: interactions with human skin cells. *Chem Biol Interact.* **2018**;295:38–51. doi:10.1016/j.cbi.2017.06.018
32. Maurer-Jones MA, Gunsolus IL, Murphy CJ, Haynes CL. Toxicity of engineered nanoparticles in the environment. *Anal Chem.* **2013**;85:3036–3049. doi:10.1021/ac303636s
33. Fard JK, Jafari S, Eghbal MA. A review of molecular mechanisms involved in toxicity of nanoparticles. *Adv Pharm Bull.* **2015**;5:447–454. doi:10.15171/apb.2015.061
34. Ong KJ, MacCormack TJ, Clark RJ, et al. Widespread nanoparticle-assay interference: implications for nanotoxicity testing. *PLoS One.* **2014**;9:e90650.
35. Lai JCK, Lai MB, Jandhyam S, et al. Exposure to titanium dioxide and other metallic oxide nanoparticles induces cytotoxicity on human neural cells and fibroblasts. *Int J Nanomedicine.* **2008**;3:533–545. doi:10.2147/ijn.s3234
36. Liu N, Tang M, Ding J. The interaction between nanoparticles-protein Corona complex and cells and its toxic effect on cells. *Chemosphere.* **2020**;245:125624. doi:10.1016/j.chemosphere.2019.125624
37. Kim H, Choi J, Lee H, et al. Skin corrosion and irritation test of nanoparticles using reconstructed three-dimensional human skin model, EpiDerm TM. *Toxicol Res.* **2016**;32:311–316. doi:10.5487/TR.2016.32.4.311
38. Roslon M, Jastrzębska A, Sitarz K, et al. The toxicity in vitro of titanium dioxide nanoparticles modified with noble metals on mammalian cells. *Int J Appl Ceram Technol.* **2019**;16:481–493. doi:10.1111/ijac.13128
39. Gholinejad Z, Khadem Ansari MH, Rasmi Y. Titanium dioxide nanoparticles induce endothelial cell apoptosis via cell membrane oxidative damage and p38, PI3K/Akt, NF-κB signaling pathways modulation. *J Trace Elem Med Biol.* **2019**;54:27–35. doi:10.1016/j.jtemb.2019.03.008
40. Yin JJ, Liu J, Ehrenshaft M, et al. Phototoxicity of nano titanium dioxides in HaCaT keratinocytes-Generation of reactive oxygen species and cell damage. *Toxicol Appl Pharmacol.* **2012**;263:81–88. doi:10.1016/j.taap.2012.06.001
41. Shukla RK, Kumar A, Gurbani D, Pandey AK, Singh S, Dhawan A. TiO₂ nanoparticles induce oxidative DNA damage and apoptosis in human liver cells. *Nanotoxicology.* **2013**;7:48–60.
42. Botelho M, Costa C, Silva S, et al. Effects of titanium dioxide nanoparticles in human gastric epithelial cells in vitro. *Biomed Pharmacother.* **2014**;68:59–64. doi:10.1016/j.biopha.2013.08.006
43. Vandebriel RJ, Vermeulen JP, van Engelen LB, et al. The crystal structure of titanium dioxide nanoparticles influences immune activity in vitro and in vivo. *Part Fibre Toxicol.* **2018**;15:1–12. doi:10.1186/s12989-018-0245-5
44. Zeiss CJ. The apoptosis-necrosis continuum: insights from genetically altered mice. *Vet Pathol.* **2003**;40:481–495. doi:10.1354/vp.40-5-481
45. Elmore S. Apoptosis: a review of programmed cell death. *Toxicol Pathol.* **2007**;35:495–516. doi:10.1080/01926230701320337
46. Park E, Yi J, Chung K-H, et al. Oxidative stress and apoptosis induced by titanium dioxide nanoparticles in cultured BEAS-2B cells. *Toxicol Lett.* **2008**;180:222–229. doi:10.1016/j.toxlet.2008.06.869